Supporting Information:

Title: **Gatekeeper-activation loop cross-talk determine distinct autoactivation states of Symbiosis Receptor Kinase**

Authors' names: **Avisek Bhattacharya[a, 1], Anindita Paul[a, b, 1], Dipanjan Chakrabarti[a], Maitrayee DasGupta[a, *].**

Addresses: [a] Department of Biochemistry, University of Calcutta, Kolkata, India.

[b] Present address: Molecular Biophysics Unit, Indian Institute of Science, Bangalore, India.

[1]These authors contributed equally.

*Corresponding author.

Table of contents:

Supporting Materials and Methods:

Cloning, mutagenesis and expression of recombinant *Ah*SYMRK

The kinase domain of *Ah*SYMRK (residues 573-883) was PCR amplified from its full length cDNA template (residues 1-926), using forward and reverse primers as listed in Table S2, containing a *EcoRI* and *HindIII* site, respectively. The amplified gene was then cloned into pET28a vector (Kan, Novagen) to generate His_6-tagged *Ah*SYMRK-KD. Point mutations were generated on this template using the QuikChange Site-Directed mutagenesis kit (Stratagene). The list of primers used to generate the mutant *Ah*SYMRK-KD clones are provided in Supporting information (Table. S2). Recombinant *Ah*SYMRK-Y670F-S757A construct was cloned in pET28a vector with a C-terminal Flag-tag. Additionally, *Ah*SymRK-K625E was cloned in pET32a (Amp, Novagen) to generate the N-terminal thioredoxin tagged Trx-K625E. Sequential mutagenesis was adopted to generate the double mutants. First the *Ah*SYMRK-Y670F was generated; the mutation was verified by sequencing and then a second round of mutagenesis was performed on this template, using corresponding primers for S754A, S757A and T763A (as listed in Table S2). The His_6-tag fused kinase domain vector constructs of *Ah*SYMRK-KD was expressed for 4h in *Escherichia coli* strain BL21 (DE3) cells at 25°C with 0.5mM IPTG induction. *Ah*SYMRK-Y670F-S757A was expressed as a Flag-tagged polypeptide, as we were not able to purify it in a soluble fraction using His_6-tagged vector system. The Flag-tagged protein was also expressed under similar conditions as described. The expressed proteins were affinity-purified using Ni-NTA Superflow resin (Qiagen) under non-denaturing conditions as per manufacturer's protocol. The native proteins were subsequently dialysed against 20mM HEPES pH 7.4, 1mM EDTA, 10% glycerol and stored in aliquots at -80°C. Protein concentrations were determined using Bradford method (*1*). All the kinase domain constructs (containing residues

573-883), expressed in pET28a, migrated in denaturing SDS-PAGE as 43 kDa polypeptides, while Trx-K625E migrated as 55 kDa polypeptide.

In vitro kinase assay

Autophosphorylation and Trx-K625E phosphorylation were performed as described previously [16, 59, 60]. In general, for autophosphorylation 2-3µg of His_6-*Ah*SYMRK was incubated for 15 min in 40 mM HEPES pH 7.4 supplemented with 10mM $Mg(OAc)_2$ and [γ-^{32}P]ATP (25µM, 3000 cpm/pmol) in a reaction volume of 25µl at 25°C. For trans-autophosphorylation, 2-3µg of Trx-K625E was incubated with 2-3µg of His_6-*Ah*SYMRK-KDs (WT, Y670F, S754A, S757A, Y670F-S754A) under similar reaction conditions (40 mM HEPES pH7.4, 10mM $Mg(OAc)_2$ and [γ-^{32}P]ATP (200µM, 3000 cpm/pmol)).

In vitro phosphatase assays and rephosphorylation assay

Recombinant calf intestinal alkaline phosphatase (CIAP, Fermentas) was incubated with 10–15 µg of *Ah*SYMRK-KDs (WT and indicated mutants) at 25°C in 200µl reaction volume for 2h. For rephosphorylation experiments, the phosphatase-treated kinase polypeptides were individually affinity-purified using Ni-NTA Superflow resin (Qiagen) under non-denaturing conditions as per manufacturer's protocol. This was done to remove the phosphatase after the digestion. Dialysis conditions and protein concentrations were estimated as described previously. Rephosphorylation assays (both auto and MBP-substrate) with CIAP-treated polypeptides were performed under similar conditions as described previously.

9. Liquid chromatography-tandem mass spectrometry (LC-MS/MS) analysis

LC-MS/MS analyses of *Ah*SYMRK polypeptides was performed using an Easy nLC 1000 liquid chromatograph coupled to an ETD-equipped LTQ Orbitrap Elite mass spectrometer (Thermo Scientific, www.thermoscientific.com). Sample preparation, data acquisition and analysis were performed as described previously [15].

Materials for mass spectrometry analysis

Formic acid (ACS reagent grade) and acetonitrile (HPLC grade) were obtained from Sigma-Aldrich (www.sigmaaldrich.com). A High-Q 103S water purification system (www.high-q.com) was used to distill and purify water. The remaining reagents and chemicals were purchased from Sigma-Aldrich-Fluka (www.sigmaaldrich.com) or Thermo Fisher Scientific (www.thermofisher.com).

Sample preparation: Protein digestion and phosphopeptide enrichment

Gel bands were subjected to in-gel tryptic digestion with sequencing-grade modified trypsin was from Promega (www.promega.com) and peptide extraction was done (*2*). Extracted peptides were stored at -20°C till further analysis was performed. The peptides were either directly analyzed by LC/MS/MS or were subjected to phosphopeptide enrichment using immobilized metal affinity chromatography (IMAC) and TiO_2 affinity chromatography and subsequently analyzed by LC/MS/MS. For IMAC enrichment, peptides were resolubilized in 2% acetic acid, next applied onto 75 µl Fe-NTA agarose slurry packed within a fritted pipette tip and then washed with 100 µl of 2% acetic acid (*3*). This is followed by a more stringent wash with 100 µl of 74/25/1 100mM sodium chloride/acetonitrile/acetic acid (v/v/v), followed by a wash with 100 µl of water. Retained peptides were eluted with 200 µl of 5% ammonium hydroxide, then immediately acidified to pH 3 with formic acid. The eluted peptides were dried using vacuum

centrifugation and solubilized in 0.1% formic acid for LC/MS/MS analysis. The flow-through portions of the IMAC step (unbound and wash fractions) were then enriched using the TiO2 SpinTips Sample Prep Kit (Protea, proteabio.com), for additional phosphopeptides. As per manufacturer's instructions, 2 mg of TiO2 material was used per sample and was washed twice with wash solution 1 (100 µl per wash). Peptides were then applied onto the TiO_2 column, washed twice with 100 µl of wash solution 1and then twice with 100 µl of wash solution 2. Peptides retained on the column were eluted with the elution solution provided. Both eluted and unbound peptides were acidified with formic acid to pH 3, dried using vacuum centrifugation, and finally resuspended in 0.1% formic acid for LC/MS/MS analysis. Therefore, three "fractions" for each sample were prepared and analyzed by LC/MS/MS: IMAC elution, TiO_2 elution, TiO_2 flow-through.

LC-MS/MS data acquisition and analysis

Enriched peptide samples were injected onto a PepMap C18 5µm trapping column (Thermo Scientific), followed by separation by in-line gradient elution, onto a 75 µm id × 15 cm New Objective (www.newobjective.com) Self-Pack PicoFrit capillary packed with 1.7 µm BEH C18 stationary phase (Waters Corporation, www.waters.com). A linear gradient was employed for peptide separation, which was accomplished from 5 to 40% mobile phase B for over 40 min at a 300µl/min flow rate; mobile phase A was 0.1% formic acid in 2% acetonitrile while mobile phase B was 0.1% formic acid in acetonitrile.

The Orbitrap Elite mass spectrometer was operated in data-dependent mode. Ten most intense precursors were chosen for subsequent fragmentation using the following fragmentation techniques: collision-induced dissociation (CID), higher-energy collisional dissociation (HCD) or electron transfer dissociation (ETD). The precursor scan (m/z 400-2000) resolution was set to

60,000 at m/z 400 with a target value of 1×106 ions. The following conditions were set for normalized collision energy: 35% for CID and 30% for HCD. To facilitate data acquisition using HCD, the MS/MS scans were collected in the Orbitrap with a target value of 6×104 ions, while using CID or ETD, the MS/MS scans were captured in the linear ion trap with a target value of 5000. For ETD, in addition to setting the reaction time to 50ms, supplemental activation using CID was implemented. The ion of polycyclodimethylsiloxane (m/z 445.120025) was used for internal mass calibration. Monoisotopic precursor selection was set up and precursors with either a charge state of +1 or unknown charge were excluded. Additionally, fragmented precursor masses were excluded from further analysis for 60s.

Proteome Discoverer version 1.3 (Thermo Scientific) was used to process the raw data files. The resultant MS2 files were used for database searching against a custom forward and reverse *Escherichia coli* UniProt database (www.uniprot.org) appended with the wild type and mutant sequences of *Ah*SYMRK-KD, using the following parameters: precursor ion mass tolerance of 10 ppm; product ion mass tolerances of 0.6 Da for CID and ETD and 20 mmu for HCD; a maximum number of missed cleavages of 2; with a fixed carbamidomethylation of Cys residues and variable modifications being oxidation on Met and phosphorylation on Ser, Thr, and Tyr. The integrated Percolator node was employed to filter the searched results, using a FDR <5%. The integrated phosphoRS node was used to calculate phosphorylation site probabilities and pRS score, while the Peak Area node was used to extract the peak areas for each peptide. The cumulative peak area for each peptide were calculated by summing up the peak areas obtained across all injections for a given sample, and subsequently used for relative quantitation (*4*). Coefficient of variation (CV) values was calculated to be 12% for wild type and gatekeeper mutants. This simply implied that the abundance of each sample (wild-type or mutant) was

relatively the same, ensuring that the quantification of each peptide was accurate. To be considered for relative quantitation, a given affected phosphopeptide (as listed in Fig 2A) had to have a phosphoRS score of >60%. Normalization was done for a particular phosphopeptide against the most abundant affected phosphopeptide in WT (pS754) using the following: x/WTx_{754}, where x is the intensity of an affected phosphopeptide across all conditions and WTx_{754} is the intensity for the phosphopeptide pS754 in WT. The relative quantitation data can be found in supporting information (Table. S1).

Table. S1: List of affected phosphopeptides of *Ah*SYMRK and its gatekeeper (Y670) mutants as detected and quantitated by LFQMS (data re-analyzed from *Saha et al., 2016*).

Phosphosites	Phosphopeptide[a,b]	Summed Abundance[c]				
		WT	Y670T	Y670F	Y670A	Y670E
pS631	628 SAT**pS**TQGTR 636	2546170	515100	26710	0	
pS754	747 YAPQEGD**pS**NVSLEVR 761	2858000000	1918100000			
pS757	747 YAPQEGDSNV**pS**LEVR 761	264892000	268250000	12603940000	9800600000	4385735000
pT763	762 G**pT**AGYLDPEYYTTQQLSEK 780	2661960000	2996790000	354276000	387140000	1476100
pY766	762 GTAG**pY**LDPEYYTTQQLSEK 780	435250000	293630000			
pT763, pY771	762 G**pT**AGYLDPE**pY**YTTQQLSEK 780	897100	562300			
pT763, pY772	762 G**pT**AGYLDPEY**pY**TTQQLSEK 780	116397100	0			
pT763, pT773	762 G**pT**AGYLDPEYY**pT**TQQLSEK 780	248170000	80846000			
pY766, pT773	762 GTAG**pY**LDPEYY**pT**TQQLSEK 780	28160000	17950000			
pY772, pT773	762 GTAGYLDPEY**pY**pT**TQQLSEK 780	44760000	6578700			
pT773	762 GTAGYLDPEYY**pT**TQQLSEK 780	2651230000	1782740000	512850000	362860000	736500
pS810	807 NEW**pS**LVEWAK 816	415460000	386877000	71342000	33531000	473200
		Normalized Abundance[d]				
		WT	Y670T	Y670F	Y670A	Y670E
pS631	628 SAT**pS**TQGTR 636	0.000890892	0.00018023	9.35E-06	0	0
pS754	747 YAPQEGD**pS**NVSLEVR 761	1	0.67113366	0	0	0
pS757	747 YAPQEGDSNV**pS**LEVR 761	0.092684395	0.09385934	4.410056	3.429181	1.534547
pT763	762 G**pT**AGYLDPEYYTTQQLSEK 780	0.931406578	1.04856193	0.123959	0.135458	0.000516
pY766	762 GTAG**pY**LDPEYYTTQQLSEK 780	0.152291812	0.10273968	0	0	0
pT763, pY771	762 G**pT**AGYLDPE**pY**YTTQQLSEK 780	0.000313891	0.00019675	0	0	0
pT763, pY772	762 G**pT**AGYLDPEY**pY**TTQQLSEK 780	0.040726767	0	0	0	0
pT763, pT773	762 G**pT**AGYLDPEYY**pT**TQQLSEK 780	0.08683345	0.02828761	0	0	0
pY766, pT773	762 GTAG**pY**LDPEYY**pT**TQQLSEK 780	0.009853044	0.00628062	0	0	0
pY772, pT773	762 GTAGYLDPEY**pY**pT**TQQLSEK 780	0.015661302	0.00230185	0	0	0
pT773	762 GTAGYLDPEYY**pT**TQQLSEK 780	0.927652204	0.62377187	0.179444	0.126963	0.000258
pS810	807 NEW**pS**LVEWAK 816	0.14536739	0.13536634	0.024962	0.011732	0.000166

[a]For a phosphopeptide to be considered, it had to have a phospho RS score of >60% in at least one sample.
[b]Residues indicated in 'bold' within the phosphopeptides listed above are the sites represented in Figure 2B.
[c]For Summed abundance: Blank cells= not detected; 0= detected, but not measurable.
[d]Normalization was done against the most abundant affected phosphopeptide in WT (pS754) using the equation x/WTx_{754}, where x is the intensity of an affected phosphopeptide across all conditions and WTx_{754} is the intensity for the phosphopeptide pS754 in WT.

Table.S2: List of Primers used for mutagenesis*.

Primer	**Sequence** (5'→3')
S631A Fwd	CAGCCACGGCGACTCAG
S631A Rev	CTGAGTCGCCGTGGCTG
S754A Fwd	GAAGGAGACGCTAATGTTTC
S754A Rev	GAAACATTAGCGTCTCCTTC
S757A Fwd	GACAGTAATGTTGCACTTGAAGTAAG
S757A Rev	CTTACTTCAAGTGCAACATTACTGTC
T773A Fwd	GTAAGAGGAGCTGCGGGCTATT
T773A Rev	AATAGCCCGCAGCTCCTCTTAC
S810A Fwd	CGAAATGAGTGGGCCTTGGTTGAATGGG
S810A Rev	CCCATTCAACCAAGGCCCACTCATTTCG
*Ah*SYMRK-KD fwd	CCGGAATTCAGCAAAGATGATTTCTTC
*Ah*SYMRK-KD rev	GCCGCCCAAGCTTCATGTACTCAGATGCATT

*Primer sequences of K625E, Y670F, T763A, Y766F, Y771F and Y772F are available in *Samaddar et al., 2013*. Primer sequence of Y670E is available in *Paul et al., 2014* (5). Primer sequences of Y670T and Y670A are available in *Saha et al., 2016*.

Table.S3: Phosphorylation sites of respective protein kinases included in sequence alignment (represented in Fig. 5).

Protein kinases	Citation
*Hs*SRC	(*6*)
*Hs*LCK	(*7*)
*Hs*IGF1R	(*8, 9*)
*Hs*FGFR1	(*10*)
*Hs*P38δ	(*9, 11*)
*Hs*ERK1	(*9*)
*Hs*CDK1	(*12*)
*Hs*PKA	(*13*)
*Hs*AKT1	(*14-16*)
*Hs*PKG1	(*9, 17*)
*Hs*CAMK1	(*9, 18*)
*Hs*CAMK4	(*19*)
*Hs*IKKβ	(*20, 21*)
*Hs*Aurora A	(*9, 22, 23*)
*Hs*MEK1	(*24*)
*Hs*HPK1	(*25, 26*)
*Hs*MLK1	(*27*)
*Hs*ZAK	(*28*)
*Hs*TAK1	(*29, 30*)
*Hs*IRAK4	(*31*)
*At*BRI1	(*32, 33*)
*At*BAK1	(*34*)
*Mt*LYK3	(*35*)
*At*BIK1	(*36, 37*)
*Lj*SYMRK	(*38*)
*Ah*SYMRK	(*39, 40*)

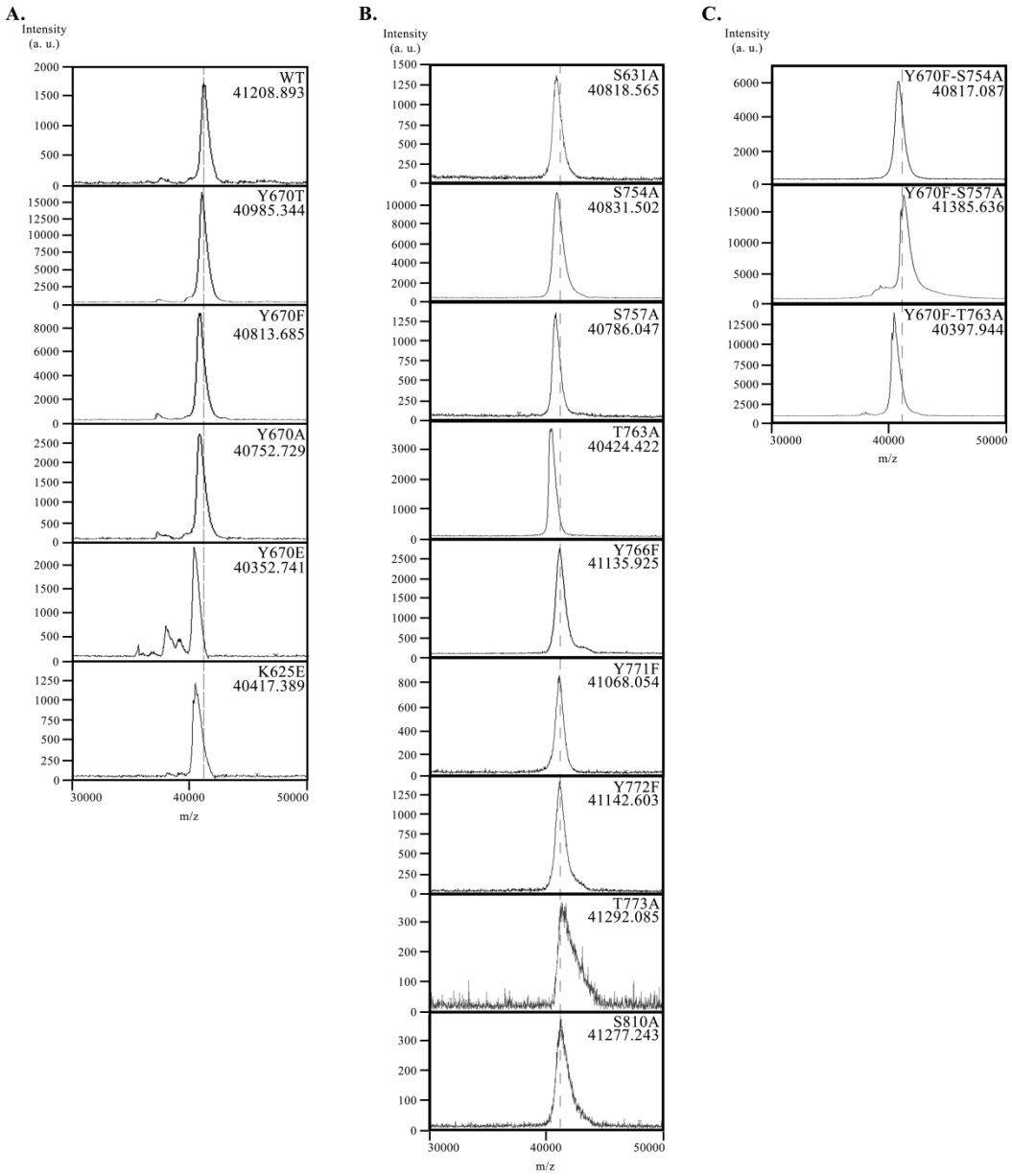

Fig S1: MALDI-TOF analysis of intact recombinant *Ah*SYMRK and the mutant kinases. Deconvoluted mass spectra in the range of *m/z* 30,000-50,000 have been shown for the following intact polypeptides. The corresponding molecular weights have also been indicated. The dotted line represents the mass for *Ah*SYMRK-WT protein and reflects the shift of spectral peaks for the mutants in different states of auto activation. **A**, *Ah*SYMRK-WT and gatekeeper mutants (Y670T/F/A/E) and K625E; **B**, single mutants S631A, S754A, S757A, T763A, Y766F, Y771F, Y772F, T773A, S810A; **C**, double mutants Y670F-S754A, Y670F-S757A, Y670F-T763A.

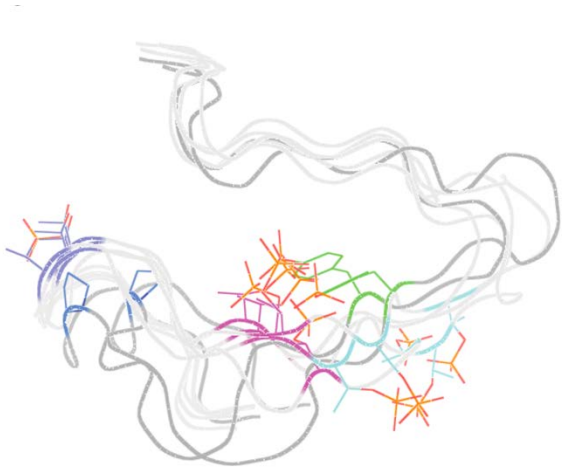

Fig S2: Superimposition of kinase activation segments: Overlay of ribbon structures of kinases chosen from Fig. 5 showing the positions of phosphorylation sites on the activation segments. Kinases with phosphorylation at sites DFG +7 to +11 are indicated in green [LCK- PDB ID: 3LCK (*41*), IGF1R- PDB ID: 1K3A (*8*)]; kinases with phosphorylation sites at APE −7 to −12 are indicated in pink (those interacting with basic Arg) and in cyan (those who do not interact with Arg) [PKA- PDB ID: 1ATP (*42*), Aur A- PDB ID: 1OL5 (*43*), IRAK4- PDB ID: 2O8Y (*44*), BRI1- PDB ID: 5LPV (*45*) and BAK1- PDB ID: 3UIM (*46*)]; phosphorylation sites in TxxY motif are indicated in violet (for Tyr kinases, LCK and IGF1R, respective Pro residues are indicated in blue).

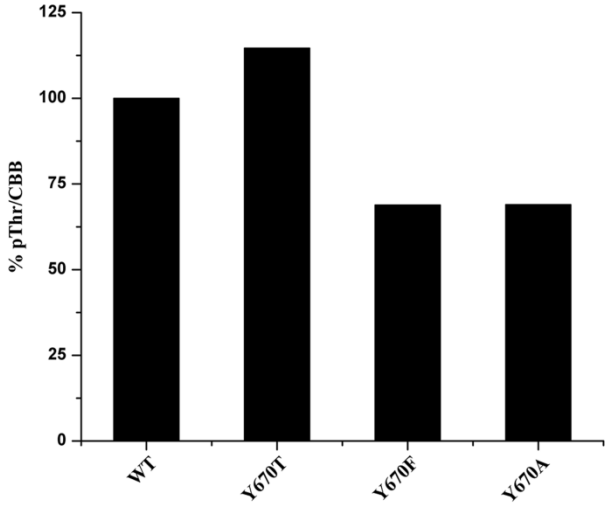

Fig S3: *Ah*SYMRK State I polypeptides have reduced Thr phosphorylation levels than State II polypeptides. Densitometric analysis of bands presented in immunoblot Fig 1A. Ratios of intensities of pThr and Coomassie Blue were performed for State II (WT and Y670T) and State I (Y670F/A) polypeptides using ImageJ.

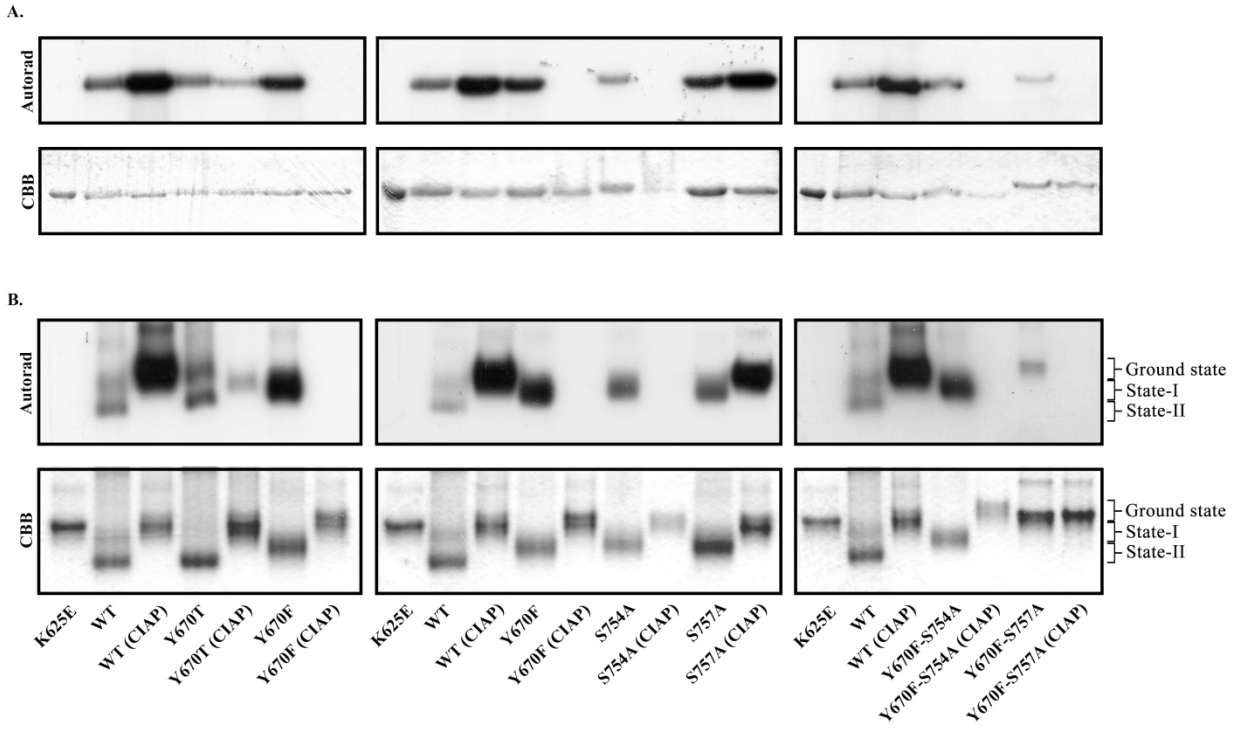

Fig S4: Differential *in vitro* autophosphorylation activities of phosphatase treated *Ah*SYMRK polypeptides. (A) Autoradiograph showing *in vitro* autophosphorylation activities of *Ah*SYMRK WT and mutants polypeptides analysed in SDS-PAGE (A) and in Native-PAGE (B).

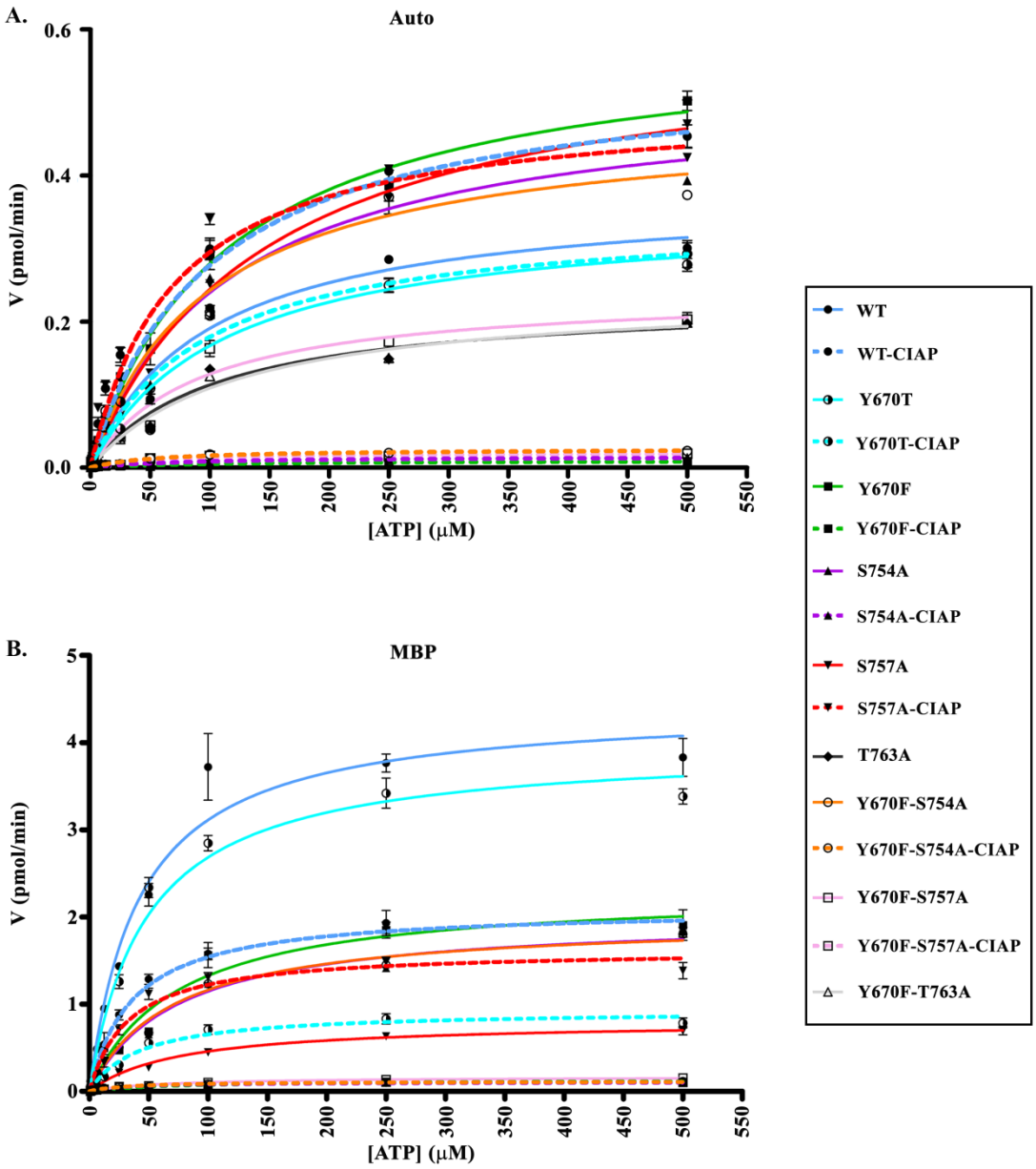

Fig S5: Kinetic characteristics of phosphatase-treated *Ah*SYMRK polypeptides. (A) Michaelis-Menten kinetics of CIAP-treated *Ah*SYMRK-WT and mutants were determined for autophosphorylation by plotting initial velocity (pmol.min-1) against varied ATP concentration (μM) as indicated in the x-axis, the error bars represent standard error of the mean (n = 3). (B) Similar kinetics of CIAP-treated *Ah*SYMRK-WT and mutant proteins were determined for substrate phosphorylation at a fixed MBP concentration, the error bars represent standard error of the mean (n = 3). Previously determined kinetics of CIAP-untreated *Ah*SYMRK polypeptides were used as reference.

Table-S4: Steady-state kinetic parameters of wild-type CIAP-treated *Ah*SYMRK and its mutant polypeptides.

Autophosphorylation	K_m (μM)	V_{max} (pmol/min)	k_{cat} (min^{-1})	k_{cat}/K_m ($M^{-1}min^{-1}$)
WT-CIAP	**98.53 ± 18.04**	**0.550 ± 0.036**	**0.02200 ± 0.0014**	**223**
Y670T-CIAP	**94.24 ± 19.99**	**0.347 ± 0.026**	**0.01390 ± 0.0010**	**147**
Y670F-CIAP	**86.80**	**0.009**	**0.00039**	**4**
S754A-CIAP	**78.47**	**0.015**	**0.00061**	**8**
S757A-CIAP	**70.11 ± 16.69**	**0.501 ± 0.039**	**0.02006 ± 0.0016**	**286**
Y670F-S754A-CIAP	**58.80**	**0.026**	**0.00104**	**18**
Y670F-S757A-CIAP	**48.36**	**0.021**	**0.00082**	**17**
Substrate phosphorylation	K_m (μM)	V_{max} (pmol/min)	k_{cat} (min^{-1})	k_{cat}/K_m ($M^{-1}min^{-1}$)
WT-CIAP	**36.49 ± 4.07**	**2.1010 ± 0.0678**	**0.08404 ± 0.0027**	**2303**
Y670T-CIAP	**42.57 ± 6.12**	**0.9301 ± 0.0399**	**0.03720 ± 0.0016**	**874**
Y670F-CIAP	**69.24**	**0.1303**	**0.0052**	**75**
S754A-CIAP	**33.22**	**0.1080**	**0.0043**	**130**
S757A-CIAP	**33.08 ± 4.55**	**1.6260 ± 0.0634**	**0.06504 ± 0.0025**	**1966**
Y670F-S754A-CIAP	**34.34**	**0.1166**	**0.0046**	**135**
Y670F-S757A-CIAP	**37.76 ± 5.30**	**0.1141 ± 0.0047**	**0.00456 ± 0.0002**	**121**

References:

1. Bradford, M. M. (1976) A rapid and sensitive method for the quantitation of microgram quantities of protein utilizing the principle of protein-dye binding, *Analytical biochemistry 72*, 248-254.
2. Mitra, S. K., Goshe, M. B., and Clouse, S. D. (2011) Experimental analysis of receptor kinase phosphorylation, In *Plant Signalling Networks*, pp 1-15, Springer.
3. Chien, K.-y., Liu, H.-C., and Goshe, M. B. (2011) Development and Application of a Phosphoproteomic Method Using Electrostatic Repulsion-Hydrophilic Interaction Chromatography (ERLIC), IMAC, and LC–MS/MS Analysis to Study Marek's Disease Virus Infection, *Journal of proteome research 10*, 4041-4053.
4. Ahmed, S., Grant, K. G., Edwards, L. E., Rahman, A., Cirit, M., Goshe, M. B., and Haugh, J. M. (2014) Data-driven modeling reconciles kinetics of ERK phosphorylation, localization, and activity states, *Molecular systems biology 10*, 718.
5. Paul, A., Samaddar, S., Bhattacharya, A., Banerjee, A., Das, A., Chakrabarti, S., and DasGupta, M. (2014) Gatekeeper tyrosine phosphorylation is autoinhibitory for Symbiosis Receptor Kinase, *FEBS letters 588*, 2881-2889.
6. Zhang, Y., Tu, Y., Zhao, J., Chen, K., and Wu, C. (2009) Reversion-induced LIM interaction with Src reveals a novel Src inactivation cycle, *The Journal of cell biology 184*, 785-792.

7. Wright, D. D., Sefton, B. M., and Kamps, M. P. (1994) Oncogenic activation of the Lck protein accompanies translocation of the LCK gene in the human HSB2 T-cell leukemia, *Molecular and Cellular Biology 14*, 2429-2437.
8. Favelyukis, S., Till, J. H., Hubbard, S. R., and Miller, W. T. (2001) Structure and autoregulation of the insulin-like growth factor 1 receptor kinase, *Nature Structural and Molecular Biology 8*, 1058.
9. Lai, S., and Pelech, S. (2016) Regulatory roles of conserved phosphorylation sites in the activation T-loop of the MAP kinase ERK1, *Molecular biology of the cell 27*, 1040-1050.
10. Mohammadi, M., Dikic, I., Sorokin, A., Burgess, W., Jaye, M., and Schlessinger, J. (1996) Identification of six novel autophosphorylation sites on fibroblast growth factor receptor 1 and elucidation of their importance in receptor activation and signal transduction, *Molecular and Cellular Biology 16*, 977-989.
11. Jiang, Y., Gram, H., Zhao, M., New, L., Gu, J., Feng, L., Di Padova, F., Ulevitch, R. J., and Han, J. (1997) Characterization of the structure and function of the fourth member of p38 group mitogen-activated protein kinases, p38δ, *Journal of Biological Chemistry 272*, 30122-30128.
12. Ducommun, B., Brambilla, P., Felix, M.-A., Franza Jr, B. R., Karsenti, E., and Draetta, G. (1991) cdc2 phosphorylation is required for its interaction with cyclin, *The EMBO journal 10*, 3311-3319.
13. Moore, M. J., Kanter, J. R., Jones, K., and Taylor, S. S. (2002) Phosphorylation of the Catalytic Subunit of Protein Kinase A AUTOPHOSPHORYLATION VERSUS PHOSPHORYLATION BY PHOSPHOINOSITIDE-DEPENDENT KINASE-1, *Journal of Biological Chemistry 277*, 47878-47884.
14. Alessi, D. R., Andjelkovic, M., Caudwell, B., Cron, P., Morrice, N., Cohen, P., and Hemmings, B. (1996) Mechanism of activation of protein kinase B by insulin and IGF-1, *The EMBO journal 15*, 6541-6551.
15. Jung, H. S., Kim, D. W., Jo, Y. S., Chung, H. K., Song, J. H., Park, J. S., Park, K. C., Park, S. H., Hwang, J. H., and Jo, K.-W. (2005) Regulation of protein kinase B tyrosine phosphorylation by thyroid-specific oncogenic RET/PTC kinases, *Molecular Endocrinology 19*, 2748-2759.
16. Zheng, Y., Peng, M., Wang, Z., Asara, J. M., and Tyner, A. L. (2010) Protein tyrosine kinase 6 directly phosphorylates AKT and promotes AKT activation in response to epidermal growth factor, *Molecular and Cellular Biology 30*, 4280-4292.
17. Pinkse, M. W., Uitto, P. M., Hilhorst, M. J., Ooms, B., and Heck, A. J. (2004) Selective isolation at the femtomole level of phosphopeptides from proteolytic digests using 2D-NanoLC-ESI-MS/MS and titanium oxide precolumns, *Analytical chemistry 76*, 3935-3943.
18. Haribabu, B., Hook, S., Selbert, M., Goldstein, E., Tomhave, E., Edelman, A., Snyderman, R., and Means, A. (1995) Human calcium-calmodulin dependent protein kinase I: cDNA cloning, domain structure and activation by phosphorylation at threonine-177 by calcium-calmodulin dependent protein kinase I kinase, *The EMBO journal 14*, 3679-3686.
19. Anderson, K. A., Noeldner, P. K., Reece, K., Wadzinski, B. E., and Means, A. R. (2004) Regulation and function of the CaMKIV/PP2A signaling complex, *Journal of Biological Chemistry*.
20. Huang, W.-C., Chen, J.-J., Inoue, H., and Chen, C.-C. (2003) Tyrosine Phosphorylation of I-B Kinase/by Protein Kinase C-Dependent c-Src Activation Is Involved in TNF--Induced Cyclooxygenase-2 Expression.
21. Mercurio, F., Zhu, H., Murray, B. W., Shevchenko, A., Bennett, B. L., Wu Li, J., Young, D. B., Barbosa, M., Mann, M., and Manning, A. (1997) IKK-1 and IKK-2: cytokine-activated IκB kinases essential for NF-κB activation, *Science 278*, 860-866.
22. Dodson, C. A., and Bayliss, R. (2012) Activation of Aurora-A kinase by protein partner binding and phosphorylation are independent and synergistic, *Journal of Biological Chemistry 287*, 1150-1157.

23. Walter, A. O., Seghezzi, W., Korver, W., Sheung, J., and Lees, E. (2000) The mitotic serine/threonine kinase Aurora2/AIK is regulated by phosphorylation and degradation, *Oncogene 19*, 4906.
24. Zheng, C.-F., and Guan, K.-L. (1994) Activation of MEK family kinases requires phosphorylation of two conserved Ser/Thr residues, *The EMBO journal 13*, 1123-1131.
25. Arnold, R., Patzak, I. M., Neuhaus, B., Vancauwenbergh, S., Veillette, A., Van Lint, J., and Kiefer, F. (2005) Activation of hematopoietic progenitor kinase 1 involves relocation, autophosphorylation, and transphosphorylation by protein kinase D1, *Molecular and Cellular Biology 25*, 2364-2383.
26. Wang, H., Chen, Y., Lin, P., Li, L., Zhou, G., Liu, G., Logsdon, C., Jin, J., Abbruzzese, J. L., and Tan, T.-H. (2014) The CUL7/F-box and WD repeat domain containing 8 (CUL7/Fbxw8) ubiquitin ligase promotes degradation of hematopoietic progenitor kinase 1, *Journal of Biological Chemistry 289*, 4009-4017.
27. Durkin, J. T., Holskin, B. P., Kopec, K. K., Reed, M. S., Spais, C. M., Steffy, B. M., Gessner, G., Angeles, T. S., Pohl, J., and Ator, M. A. (2004) Phosphoregulation of mixed-lineage kinase 1 activity by multiple phosphorylation in the activation loop, *Biochemistry 43*, 16348-16355.
28. Tosti, E., Waldbaum, L., Warshaw, G., Gross, E. A., and Ruggieri, R. (2004) The stress kinase MRK contributes to regulation of DNA damage checkpoints through a p38γ-independent pathway, *Journal of Biological Chemistry 279*, 47652-47660.
29. Kishimoto, K., Matsumoto, K., and Ninomiya-Tsuji, J. (2000) TAK1 mitogen-activated protein kinase kinase kinase is activated by autophosphorylation within its activation loop, *Journal of Biological Chemistry 275*, 7359-7364.
30. Sakurai, H., Miyoshi, H., Mizukami, J., and Sugita, T. (2000) Phosphorylation-dependent activation of TAK1 mitogen-activated protein kinase kinase kinase by TAB1, *FEBS letters 474*, 141-145.
31. Cheng, H., Addona, T., Keshishian, H., Dahlstrand, E., Lu, C., Dorsch, M., Li, Z., Wang, A., Ocain, T. D., and Li, P. (2007) Regulation of IRAK-4 kinase activity via autophosphorylation within its activation loop, *Biochemical and biophysical research communications 352*, 609-616.
32. Oh, M.-H., Wang, X., Kota, U., Goshe, M. B., Clouse, S. D., and Huber, S. C. (2009) Tyrosine phosphorylation of the BRI1 receptor kinase emerges as a component of brassinosteroid signaling in Arabidopsis, *Proceedings of the National Academy of Sciences 106*, 658-663.
33. Wang, X., Goshe, M. B., Soderblom, E. J., Phinney, B. S., Kuchar, J. A., Li, J., Asami, T., Yoshida, S., Huber, S. C., and Clouse, S. D. (2005) Identification and functional analysis of in vivo phosphorylation sites of the Arabidopsis BRASSINOSTEROID-INSENSITIVE1 receptor kinase, *The Plant Cell 17*, 1685-1703.
34. Wang, X., Kota, U., He, K., Blackburn, K., Li, J., Goshe, M. B., Huber, S. C., and Clouse, S. D. (2008) Sequential transphosphorylation of the BRI1/BAK1 receptor kinase complex impacts early events in brassinosteroid signaling, *Developmental cell 15*, 220-235.
35. Klaus-Heisen, D., Nurisso, A., Pietraszewska-Bogiel, A., Mbengue, M., Camut, S., Timmers, T., Pichereaux, C., Rossignol, M., Gadella, T. W., and Imberty, A. (2011) Structure-function similarities between a plant receptor-like kinase and the human interleukin-1 receptor-associated kinase-4, *Journal of Biological Chemistry*, jbc. M110. 186171.
36. Laluk, K., Luo, H., Chai, M., Dhawan, R., Lai, Z., and Mengiste, T. (2011) Biochemical and genetic requirements for function of the immune response regulator BOTRYTIS-INDUCED KINASE1 in plant growth, ethylene signaling, and PAMP-triggered immunity in Arabidopsis, *The Plant Cell*, tpc. 111.087122.

37. Xu, J., Wei, X., Yan, L., Liu, D., Ma, Y., Guo, Y., Peng, C., Zhou, H., Yang, C., and Lou, Z. (2013) Identification and functional analysis of phosphorylation residues of the Arabidopsis BOTRYTIS-INDUCED KINASE1, *Protein & cell 4*, 771-781.
38. Yoshida, S., and Parniske, M. (2005) Regulation of plant symbiosis receptor kinase through serine and threonine phosphorylation, *Journal of Biological Chemistry 280*, 9203-9209.
39. Saha, S., Paul, A., Herring, L., Dutta, A., Bhattacharya, A., Samaddar, S., Goshe, M. B., and DasGupta, M. (2016) Gatekeeper Tyrosine phosphorylation of SYMRK is essential for synchronising the epidermal and cortical responses in root nodule symbiosis, *Plant physiology*, pp. 01962.02015.
40. Samaddar, S., Dutta, A., Sinharoy, S., Paul, A., Bhattacharya, A., Saha, S., Chien, K.-y., Goshe, M. B., and DasGupta, M. (2013) Autophosphorylation of gatekeeper tyrosine by symbiosis receptor kinase, *FEBS letters 587*, 2972-2979.
41. Yamaguchi, H., and Hendrickson, W. A. (1996) Structural basis for activation of human lymphocyte kinase Lck upon tyrosine phosphorylation, *Nature 384*, 484.
42. Zheng, J., Knighton, D. R., Ten Eyck, L. F., Karlsson, R., Xuong, N.-H., Taylor, S. S., and Sowadski, J. M. (1993) Crystal structure of the catalytic subunit of cAMP-dependent protein kinase complexed with magnesium-ATP and peptide inhibitor, *Biochemistry 32*, 2154-2161.
43. Bayliss, R., Sardon, T., Vernos, I., and Conti, E. (2003) Structural basis of Aurora-A activation by TPX2 at the mitotic spindle, *Molecular cell 12*, 851-862.
44. Wang, Z., Wesche, H., Stevens, T., Walker, N., and Yeh, W.-C. (2009) IRAK-4 inhibitors for inflammation, *Current topics in medicinal chemistry 9*, 724-737.
45. Bojar, D., Martinez, J., Santiago, J., Rybin, V., Bayliss, R., and Hothorn, M. (2014) Crystal structures of the phosphorylated BRI 1 kinase domain and implications for brassinosteroid signal initiation, *The Plant Journal 78*, 31-43.
46. Yan, L., Ma, Y., Liu, D., Wei, X., Sun, Y., Chen, X., Zhao, H., Zhou, J., Wang, Z., and Shui, W. (2012) Structural basis for the impact of phosphorylation on the activation of plant receptor-like kinase BAK1, *Cell research 22*, 1304.